

CMIP5 model simulations of the Pacific meridional mode and its connection to the two types of ENSO

Chun-Yi Lin,^{a,b*} Jin-Yi Yu^c and Huang-Hsiung Hsu^a

^a *Research Center for Environmental Changes, Academia Sinica, Taipei, Taiwan*

^b *Research and Collection Division, National Museum of Marine Science and Technology, Keelung, Taiwan*

^c *Department of Earth System Science, University of California, Irvine, CA, USA*

ABSTRACT: This study examines the Pacific meridional mode (PMM) simulated in the pre-industrial simulations of the Coupled Model Intercomparison Project Phase 5 (CMIP5). The spatial pattern and intensity of the PMM were found to be reasonably simulated by CMIP5 models, as was the subtropical atmosphere–ocean coupling associated with the PMM. However, the persistence of the coupling, which sustains the PMM’s duration and extends its pattern equatorward, was found to be underestimated in most of the CMIP5 models. Many of the simulated PMMs do not have a pattern that extends far enough into the tropical Pacific to influence El Niño–Southern Oscillation (ENSO). The CMIP5 models that do produce longer persistence for the PMM coupling show a higher correlation of the PMM with the Central-Pacific (CP) type of ENSO than with the Eastern-Pacific (EP) type of the ENSO. This study concludes that (1) the PMM and its associated subtropical Pacific ocean–atmosphere coupling are important to the generation of the CP type of ENSO; (2) the so-called seasonal footprinting mechanism that sustains an equatorward extension of the PMM is not well simulated in a majority of the CMIP5 models; and (3) the persistence of the subtropical Pacific coupling is more important than the other properties in gauging a model’s skill in the PMM simulation.

KEY WORDS Pacific meridional mode; central Pacific ENSO; eastern Pacific ENSO; CMIP5 pre-industrial simulations

Received 2 March 2014; Revised 11 July 2014; Accepted 17 July 2014

1. Introduction

The Pacific meridional mode (PMM; Chiang and Vimont, 2004) is a leading mode of variability in the northeastern subtropical Pacific that is characterized by covariability in sea surface temperature (SST) and surface wind. Wind fluctuations associated with extratropical atmospheric variability induce SST anomalies in the subtropical Pacific via surface evaporation, which then feedback to modify the atmospheric winds via convection. The wind anomalies induced by the convection tend to locate to the southwest corner of the subtropical SST anomalies (Xie and Philander, 1994), where new SST anomalies can be formed through evaporation. The atmosphere then continues to respond to the new SST anomalies by producing wind anomalies further southwestward. Through this wind–evaporation–SST (WES) feedback (Xie and Philander, 1994), the SST anomalies initially induced by the extratropical atmosphere can extend southwestward from near Baja California towards the tropical central Pacific to form the spatial pattern of the PMM. The atmosphere–ocean coupling also sustains the PMM from boreal winter, when the extratropical atmospheric variability is the most active, to the following spring or

summer to excite El Niño events. Therefore, the PMM has been suggested to play an important role in connecting tropical and extratropical climate variability (Anderson, 2003; Chiang and Vimont, 2004; Chang *et al.*, 2007; Li *et al.*, 2008; Alexander *et al.*, 2010). The series of coupling processes in the subtropics that responsible for the equatorward spreading of the SST anomalies are also referred to as the seasonal footprinting mechanism (Vimont *et al.*, 2001, 2003, 2009).

These earlier studies on the relationship between the PMM and El Niño–Southern Oscillation (ENSO) did not consider the existence of different types of ENSO. Recent studies have increasingly suggested that there exists two different types of ENSO (Larkin and Harrison, 2005; Yu and Kao, 2007; Ashok *et al.*, 2007; Kao and Yu, 2009; Kug *et al.*, 2009). One is the Eastern-Pacific (EP) ENSO that has most of its SST anomalies centered in the eastern Pacific, and the other is the Central-Pacific (CP) ENSO that confines SST anomalies more to the central Pacific (Yu and Kao, 2007; Kao and Yu, 2009). It was suggested that forcing from the extratropical atmosphere may be particularly important to the generation of the CP ENSO (Yu *et al.*, 2011; Yu and Kim, 2011; Kim and Yu, 2012). Consistent with this suggestion, Kim *et al.* (2012) analysed the ENSO simulation produced by NCEP’s Climate Forecast System (CFS) model to show that the model’s performance in simulating the CP ENSO was related to its ability to simulate the PMM.

* Correspondence to: C.-Y. Lin, Research Center for Environmental Changes, Academia Sinica, 128 Academia Road, Section 2, Nankang, Taipei 11529, Taiwan. E-mail: garry7946@gmail.com

In this study, we conduct a systematic examination using the large number of model simulations available from Coupled Model Intercomparison Project Phase 5 (CMIP5) to examine how well the PMM and its associated atmosphere–ocean coupling are simulated in the CMIP5 models and whether or not the models simulated different relationships between the PMM and the two types of ENSO. Four specific metrics are developed to evaluate the models' skill in simulating the subtropical atmosphere–ocean coupling associated with the PMM. The possible influence of the skill in reproducing the PMM on the simulations of the two types of ENSO, particularly the CP type, is also examined.

2. Data and method

In this study, we analysed the pre-industrial simulations produced by 23 CMIP5 models. The names of the models are listed in Figure 2. The length of the simulations varied from model to model. The output from the last 100 years of each simulation was analysed. For the observational SSTs and surface winds, we used data from the National Centers for Environmental Prediction–National Center for Atmospheric Research (NCEP–NCAR) Reanalysis (Kalnay *et al.*, 1996; Kistler *et al.*, 2001), from 1948 to 2010. Monthly anomalies from the model simulations and the NCEP Reanalyses are calculated by removing the respective monthly mean climatology and trend. A regression-empirical orthogonal function (EOF) analysis (Kao and Yu, 2009; Yu and Kim, 2010) was applied to monthly SST anomalies to identify the EP and CP types of ENSO. With this method, we first removed the tropical Pacific SST anomalies that are regressed with the Niño 1 + 2 (0° – 10° S, 80° – 90° W) SST index and then applied the EOF analysis to the remaining SST anomalies to obtain the SST anomaly pattern for the CP ENSO. Similarly, we subtracted the SST anomalies regressed with the Niño4 (5° S– 5° N, 160° E– 150° W) SST index from the original SST anomalies before the EOF analysis was applied to identify the leading structure of the EP ENSO. The EOF patterns we obtain here are similar to those reported in Kao and Yu (2009) and Kim and Yu (2012) and are displayed in Figure 1 to aid the discussion. As shown in the figure, the EP ENSO is characterized by SST anomalies extending westward from the South American Coast towards the equatorial central Pacific, whereas the SST anomalies in the CP ENSO are confined around the International dateline and have a branch of the anomalies extending towards the northeastern subtropical Pacific. The two types of ENSO were also obtained from the pre-industrial simulations of the CMIP5 models using the same regression-EOF analysis. Their SST anomaly patterns are similar to those reported in Kim and Yu (2012; see their Figure 1) and are not shown here. Consistent with Kim and Yu (2012), the observed spatial patterns of the two types of ENSO can be reproduced in the CMIP5 models, although discrepancies exist with the observations in the detailed realism of the simulated pattern and intensity.

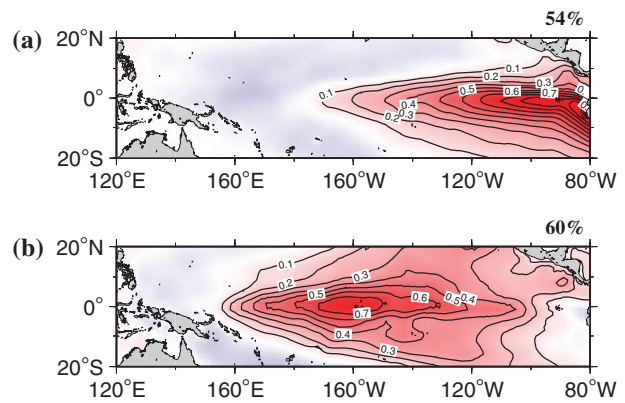


Figure 1. Spatial patterns of the first EOF mode obtained by a EOF-regression analysis method for the (a) EP ENSO and (b) CP ENSO calculated from NCEP Reanalyses. The values shown are the loading coefficients scaled by its square root of the corresponding eigenvalue to represent the standard deviation (in units of $^{\circ}$ C) of the SST anomalies associated with the mode. The percentage of variance explained by the EOF mode is indicated on top of the panels.

To identify the PMM, a singular value decomposition (SVD) analysis (Bretherton *et al.*, 1992) was applied to the cross-covariance matrix between SST and surface wind anomalies in the region between 175° E– 90° W and 20° S– 30° N to extract the leading mode of coupled variability. Following Chiang and Vimont (2004), to exclude the ENSO influence from the analysis result, the subtropical Pacific SST and wind anomalies that are regressed with the cold tongue index (SST anomalies averaged over 6° S– 6° N and 180° – 90° W) are removed before the SVD analysis is applied. It is necessary to point out that the region defined for the cold tongue index covers both the eastern and central Pacific. Therefore, by removing the regression with the cold tongue index, the influence of both the EP ENSO and CP ENSO are largely removed from the subtropical Pacific SST and wind anomalies before the SVD analysis was applied to obtain the PMM.

3. Results

We first examined in Figure 2 the leading SVD modes calculated from the CMIP5 pre-industrial simulations and the NCEP/NCAR Reanalysis, which represents the simulated and observed PMMs. The observed PMM is characterized by two main features: (1) a center of large warm SST anomalies to the southwest of Baja California and (2) a southwestward extension of these anomalies towards the central tropical Pacific. These two features are generally reproduced in most of the simulated PMM patterns, despite variations in the magnitude of the SST anomalies and their elongation towards the central tropical Pacific. Here, the realism of the simulated PMM patterns can be examined by calculating their pattern correlations with the PMM obtained from the NCEP Reanalysis over the domain of the figure. Figure 3(a) shows that the pattern correlations between the simulated PMMs and the observed PMM are larger than 0.7 for all the CMIP5 models, except

PACIFIC MERIDIONAL MODE AND ITS CONNECTION WITH ENSO

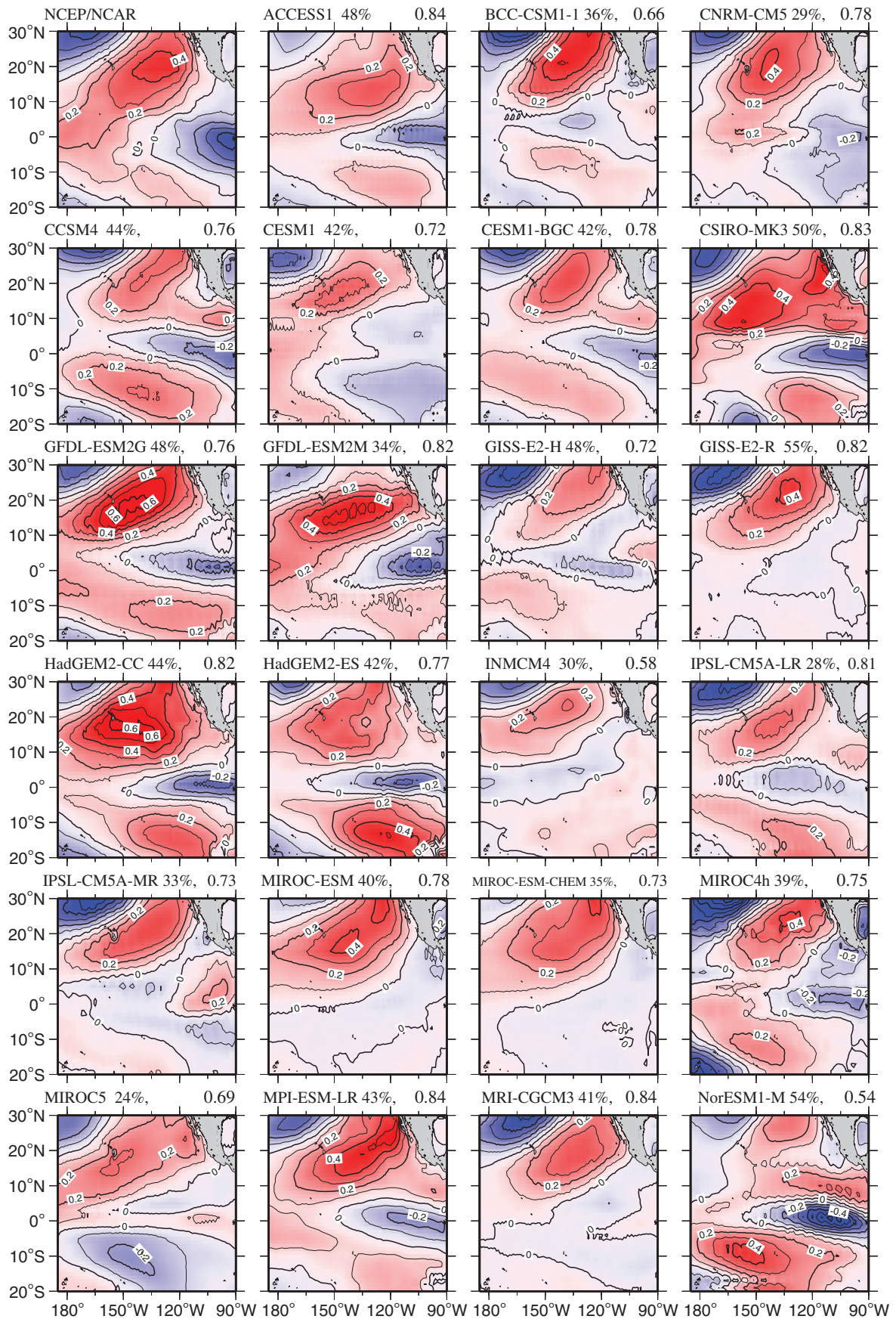


Figure 2. The SST variability pattern of the PMM calculated from NCEP Reanalyses and 23 CMIP5 models. The patterns were obtained from an SVD analysis, and the loading coefficients have been scaled by the eigenvalues of the SVD modes. Also shown on top of each panel is the pattern correlation (right) between model and NCEP Reanalyses and the explained variance (left, in %).

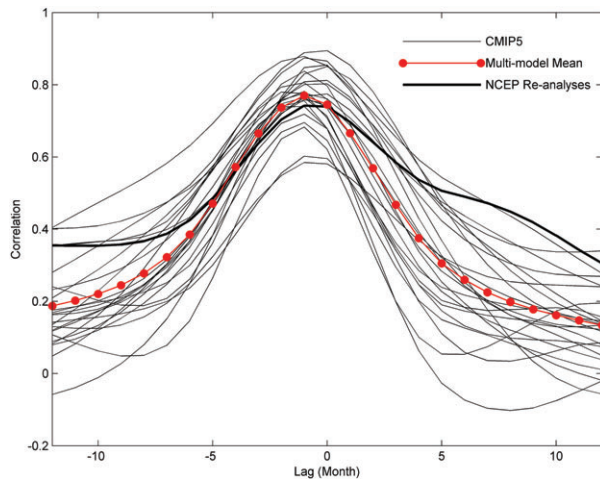


Figure 4. Lead-lag correlation coefficients between PMM-SST and PMM-wind index calculated from the CMIP5 models (thin lines), CMIP5 multi-model ensemble mean (dotted line) and NCEP Re-analyses (thick black line). Negative lags indicate that the PMM-wind leads the PMM-SST.

pattern correlation and the PMM intensity. The inter-model differences in the southwestward extension feature of the PMM are not well reflected in the comparisons of the PMM pattern correlation and intensity. In the observed PMM, the warm SST anomalies extend deep into the central tropical Pacific. In the simulated PMMs, the SST anomalies do not necessarily extend as far into the tropics (Figure 2). Also, the exact longitude at which the SST anomalies enter the tropics varies from model to model. As noted in the introduction, the southwestward extension of the PMM-SST anomalies, which is the link between PMM and ENSO, is a result of the SST-wind coupling over the subtropical Pacific. Variations in the model simulations of the southwestward extension, therefore, imply diverse characteristics in the subtropical coupling in the models, as well as the possibility of differing PMM-ENSO relations in their simulations. Next, we will discuss more characteristics of the PMM air-sea coupling with ENSO and the uncertainty in the CMIP5 model.

We consider two aspects of the subtropical Pacific ocean-atmosphere coupling can be crucial to the southwestward extension of the PMM. One is the strength of the coupling between SST and surface wind, and the other is the persistence of the coupling. We first examine the coupling strength. The SVD analysis used to identify the spatial pattern of the PMM also produces a pair of principal components (PCs) for the leading SVD mode. These PCs represent the temporal variations of the PMM-associated SST and surface wind anomalies. The correlation between these two PCs can be used to quantify the strength of the atmosphere-ocean coupling. Figure 4 shows the lead-lag correlation between these two PCs calculated from the leading SVD modes of the CMIP5 simulations and the NCEP/NCAR Reanalysis. For the observed PMM (the thick solid line), the maximum correlation coefficient occurs when the surface wind PC leads the

SST-PC by about 1 month (i.e. at lag -1), which reflects the wind-driven nature of the PMM-SST variability. The maximum correlation then decays slowly at positive lags, which indicates the persistence of the coupling from the SST feedback. The lead-lag correlations calculated from the simulated PMMs are, in general, close to the observed correlations. However, the maximum value and decay rate of the correlation varies pretty widely among the models. Figure 3(c) displays the maximum correlation coefficients taken from Figure 4, which is referred to as the PMM coupling strength. It shows that, in general, the CMIP5 models overestimate the subtropical coupling strength with the ensemble model mean strength larger than the observed strength (approximately 0.75).

A different picture emerges when we examined the persistence time of the PMM coupling, which is calculated as the time (i.e. lag) for the maximum correlation coefficient to decay to its $1/e$ value. Figure 3(d) displays the persistence times calculated from Figure 4. It shows that all the CMIP5 models underestimate the coupling persistence time, which is about 11 months in the NCEP Reanalyses. The ensemble mean is only about 6.5 months. The four models that produce the shortest persistence time (i.e. GISS-E2-H, IPSL-CM5A-MR, CESM1-BGC, INMCM4) all produce a PMM pattern whose southwestward extension is relatively weak below 10°N (see Figure 2). In contrast, for the six models that produce the longest persistence time (i.e. HadGEM2-CC, HadGEM2-ES, MIROC5, MIROC-ESM, MIROC-ESM-CHEM, and GFDL-ESM2G), their PMM patterns extended deep into the central tropical Pacific. It seems that the persistence of the PMM coupling determines whether or not a PMM structure can extend realistically far into the tropics. Therefore, the coupling persistence time is likely the most important property of the PMM in determining the connections of the PMM with the ENSO.

Finally, we examined the relationships between the PMM and the two types of ENSO in 23 CMIP5 model simulations. As mentioned in Section 2, a regression-EOF method was used to characterize the CP and EP types of ENSO from the simulations and NCEP Reanalyses. The PCs from the analyses represent the variations in the intensity of the two types of ENSO and are referred to as the CP Index and the EP Index. We first examined the relationships between the PMM and the two types of ENSO by calculating the correlation between the EP/CP Index and the SST-PC of the PMM mode. We then linked the PMM-CP/EP ENSO correlations to the PMM intensity, spatial pattern, coupling strength, and persistence time. It was found that of these features the simulated PMM-CP ENSO correlation is most closely associated with the PMM persistence time. As shown in Figure 5(a), the CMIP5 models that produce a longer PMM persistence time tend to show a stronger correlation between the PMM and the CP ENSO. The correlation between these two quantities is as high as 0.71 across the 23 CMIP5 models we analysed, which is statistically significant at the 95% level based on F -test. This high tendency supports our previous assertion that the persistence time determines

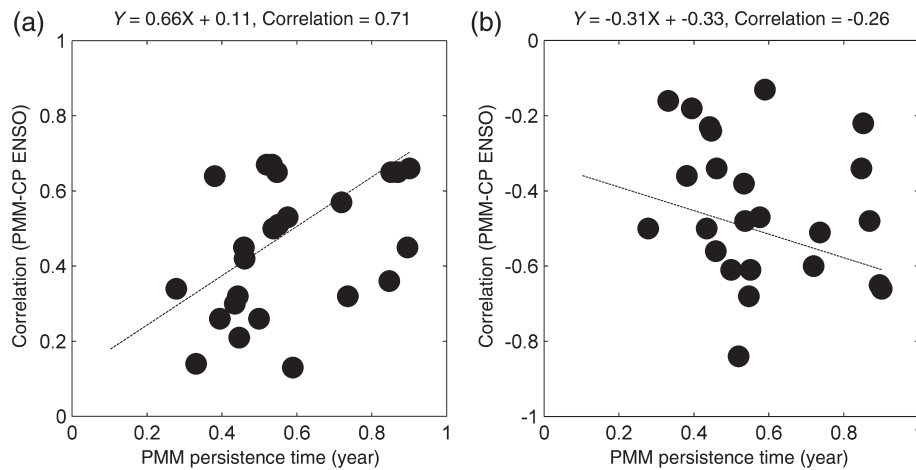


Figure 5. Scatter plots of the CMIP5 models between their PMM persistence time and the PMM-ENSO correlation for (a) the CP ENSO and (b) the EP ENSO. The best fitting line is represented by the dashed lines.

how deeply the PMM can penetrate into the tropics to influence the CP ENSO. However, a similar robust relationship cannot be found between the simulated PMM persistence time and the simulated PMM-EP ENSO correlation among the CMIP5 models. As shown in Figure 5(b), the simulated PMM-EP ENSO correlation can vary over a wide range of values for a similar PMM persistence time. Therefore, the PMM-ENSO relationship is affected by the PMM persistence time only for the CP type but not for the EP type of ENSO. It should be noted that, since the coupling persistence time are underestimated in the models than in the reanalysis (cf. Figure 3(d)), the multi-model mean value of the PMM-CP ENSO correlation (0.44) is lower than the correlation calculated from the reanalysis (0.67).

4. Conclusion

The PMM is a leading mode of coupled atmosphere–ocean variability in the subtropical Pacific and may play a crucial role in transmitting extratropical forcing into the tropics to impact ENSO activity. In this study, we examine the simulation of the PMM in 23 CMIP5 models, with a particular focus on the properties of its associated ocean–atmosphere coupling and its connection to the two types of ENSO. By examining four properties of the PMM, our analysis show more evidence that it is the persistence time of PMM’s associated atmosphere–ocean coupling in the subtropics that is most challenging for the CMIP5 models to simulate. We also suggested that the persistence time of the coupling is more important than the other properties of the PMM in connecting the PMM and the CP type of ENSO. It is a conclusion of this study that the persistence time of the PMM should be considered as the most important metric for gauging model performance in the PMM simulation. Our findings that more persist PMMs are associated with stronger PMM-CP ENSO correlation in the CMIP5 models also lend support to the suggestion that the PMM contributes to the generation of the CP ENSO. All these

findings suggest that the so-called seasonal footprinting mechanism (Vimont *et al.*, 2001, 2003) – responsible for sustaining the PMM from boreal winter to the following spring or summer – is not well simulated in the contemporary models. This deficiency can affect the model’s simulation of extratropical–tropical interactions, as well as the simulation of the two types of ENSO and is suggested as an area of focus for further model improvement. It is necessary to note that CMIP models are known to suffer an excessive cold tongue problem in the equatorial eastern Pacific (e.g. Zheng *et al.*, 2012; Li and Xie, 2014), which may affect their ability to realistically simulate the EP ENSO. The weak PMM-EP ENSO relation found here might also be linked to this model bias.

Acknowledgements

We thank three anonymous reviewers and Editor Jose Marengo for their valuable comments. This work was supported by Taiwan’s National Science Council (NSC 100-2119-M-001-029-MY5) and by the US National Science Foundation (AGS-1233542). We acknowledge the various modelling groups for producing and providing their output, the PCMDI for collecting and archiving the CMIP5 multi-model dataset, the WCRP’s WGCM for organizing the analysis activity, and the Office of Science, U.S. Department of Energy, for supporting this dataset in partnership with the Global Organization for Earth System Science Portals.

References

- Alexander MA, Vimont DJ, Chang P, Scott JD. 2010. The impact of extratropical atmospheric variability on ENSO: testing the seasonal footprinting mechanism using coupled model experiments. *J. Clim.* **23**: 2885–2901.
- Anderson BT. 2003. Tropical Pacific sea-surface temperatures and preceding sea level pressure anomalies in the subtropical North Pacific. *J. Geophys. Res.* **108**: 4732, doi: 10.1029/2003JD003805.
- Ashok K, Behera S, Rao AS, Weng H, Yamagata T. 2007. El Niño Modoki and its teleconnection. *J. Geophys. Res.* **112**: C11007, doi: 10.1029/2006JC003798.

- Bretherton CS, Smith C, Wallace JM. 1992. An intercomparison of methods for finding coupled patterns in climate data. *J. Clim.* **5**: 541–560.
- Chang P, Zhang L, Saravanan R, Vimont DJ, Chiang JCH, Ji L, Seidel H, Tippet MK. 2007. Pacific meridional mode and El Niño–Southern Oscillation. *Geophys. Res. Lett.* **34**: L16608, doi: 10.1029/2007GL030302.
- Chiang JC, Vimont D. 2004. Analogous Pacific and Atlantic meridional modes of tropical atmosphere–ocean variability. *J. Clim.* **17**: 4143–4158.
- Kalnay E, Kanamitsu M, Kistler R, Collins W, Deaven D, Gandin L, Iredell M, Saha S, White G, Woollen J, Zhu Y, Leetmaa A, Reynolds B, Chelliah M, Ebisuzaki W, Higgins W, Janowiak J, Mo KC, Ropelewski C, Wang J, Jenne R, Joseph D. 1996. The NCEP/NCAR 40-year reanalysis project. *Bull. Am. Meteorol. Soc.* **77**: 437–470.
- Kao HY, Yu JY. 2009. Contrasting eastern-Pacific and central-Pacific types of El Niño. *J. Clim.* **22**: 615–632.
- Kim ST, Yu JY. 2012. The two types of ENSO in CMIP5 models. *Geophys. Res. Lett.* **39**: L11704, doi: 10.1029/2012GL052006.
- Kim ST, Yu JY, Kumar A, Wang H. 2012. Examination of the two types of ENSO in the NCEP CFS model and its extratropical associations. *Mon. Weather Rev.* **140**: 1908–1923.
- Kistler R, Kalnay E, Collins W, Saha S, White G, Woollen J, Chelliah M, Ebisuzaki W, Kanamitsu M, Kousky V, Dool HVD, Jenne R, Fiorino M. 2001. The NCEP–NCAR 50-year reanalysis: monthly means CD-ROM and documentation. *Bull. Am. Meteorol. Soc.* **82**: 247–267.
- Kug JS, Jin FF, An SI. 2009. Two types of El Niño events: cold tongue El Niño and warm pool El Niño. *J. Clim.* **22**: 1499–1515.
- Larkin NK, Harrison DE. 2005. On the definition of El Niño and associated seasonal average U.S. weather anomalies. *Geophys. Res. Lett.* **32**: L13705, doi: 10.1029/2005GL022738.
- Li G, Xie SP. 2014. Tropical biases in CMIP5 multimodel ensemble: the excessive equatorial Pacific cold tongue and double ITCZ problems. *J. Clim.* **27**: 1765–1780.
- Li Z, Chang P, Ji L. 2008. Linking the Pacific meridional modes to ENSO: coupled model analysis. *J. Clim.* **22**: 3488–3505.
- Vimont DJ, Battisti DS, Hirst AC. 2001. Footprinting: a seasonal connection between the Tropics and mid-latitudes. *Geophys. Res. Lett.* **28**: 3923–3926.
- Vimont DJ, Wallace JM, Battisti DS. 2003. The seasonal footprinting mechanism in the Pacific: implications for ENSO. *J. Clim.* **16**: 2668–2675.
- Vimont DJ, Alexander M, Fontaine A. 2009. Midlatitude excitation of tropical variability in the Pacific: the role of thermodynamic coupling and seasonality. *J. Clim.* **22**: 518–534.
- Xie SP, Philander SGH. 1994. A coupled ocean–atmosphere model of relevance to the ITCZ in the eastern Pacific. *Tellus A* **46**: 340–350.
- Yu JY, Kao HY. 2007. Decadal changes of ENSO persistence barrier in SST and ocean heat content indices: 1958–2001. *J. Geophys. Res.* **112**: D13106, doi: 10.1029/2006JD007654.
- Yu JY, Kim ST. 2010. Identification of central-Pacific and eastern-Pacific types of El Niño in CMIP3 models. *Geophys. Res. Lett.* **37**: L15705, doi: 10.1029/2010GL044082.
- Yu JY, Kim ST. 2011. Relationships between extratropical sea level pressure variations and central-Pacific and eastern-Pacific types of ENSO. *J. Clim.* **24**: 708–720.
- Yu JY, Kao HY, Lee T, Kim ST. 2011. Subsurface ocean temperature indices for Central-Pacific and Eastern-Pacific types of El Niño and La Niña events. *Theor. Appl. Climatol.* **103**: 337–344.
- Zheng Y, Lin JL, Shinoda T. 2012. The equatorial Pacific cold tongue simulated by IPCC AR4 coupled GCMs: upper ocean heat budget and feedback analysis. *J. Geophys. Res.* **117**: C05024, doi: 10.1029/2011JC007746.